

IpaA Targets β 1 Integrins and Rho to Promote Actin Cytoskeleton Rearrangements Necessary for *Shigella* Entry^{*[S]}

Received for publication, June 21, 2006, and in revised form, August 31, 2006 Published, JBC Papers in Press, October 22, 2006, DOI 10.1074/jbc.M605939200

Kris A. DeMali^{†1}, April L. Jue[§], and Keith Burridge[§]

From the [§]Department of Cell and Developmental Biology and Lineberger Comprehensive Cancer Center, University of North Carolina, Chapel Hill, North Carolina 27599 and the [†]Department of Biochemistry, University of Iowa, Iowa City, Iowa 52242

Shigella invasion into the colonic epithelium involves many steps including the formation of large membrane protrusions by the epithelial cells that facilitate bacterial engulfment. IpaA, a *Shigella* protein secreted into target cells upon cell contact induces a loss of actin stress fibers in cells and promotes the reorganization of actin at the site of entry. The mechanism for this is not known but is thought to involve recruitment of the focal adhesion protein vinculin to IpaA. Here we have examined the mechanism for the effects of IpaA on the actin cytoskeleton. We show that IpaA-induced loss of actin stress fibers and cell rounding do not require vinculin expression or an intact vinculin binding site on IpaA. Rather, we find that cells expressing IpaA exhibited elevated Rho activity and increased myosin light chain phosphorylation. In addition, IpaA decreases integrin affinity for extracellular matrix ligands by interfering with talin recruitment to the integrin cytoplasmic tail. The combination of these two effects, namely weakened adhesion and increased contractility, account for the loss of actin stress fibers and cell rounding observed in cells exposed to IpaA.

Shigella, the causative agent of bacillary dysentery, is a Gram-negative bacterium that exerts its effects by invading the colonic mucosa. Upon entry into the epithelium of the colon, *Shigella* multiply, cause cell death, and spread laterally to infect and kill adjacent epithelial cells, inducing ulceration, inflammation, and bleeding. To facilitate entry, *Shigella* triggers *de novo* actin polymerization that drives the formation of large membrane protrusions that arise from the epithelium and evolve into a phagocytic-like cup that merges above the bacterium. These protrusions are rich in densely branched actin networks that are reorganized to allow for closure of the phagocytic cup and internalization of the bacterium. Elucidation of the molecular bases of these cytoskeletal rearrangements is essential for better understanding the mechanism of *Shigella* entry.

To facilitate invasion, the *Shigella* type III secretion system is stimulated upon contact with host cells and delivers bacterial “effector” molecules into the surrounding bacterial

space and/or host cell membrane (1). These invasins directly alter the host cell cytoskeleton and/or allow for the delivery of other type III effectors into the cytoplasm to promote invasion. For *Shigella*, these invasins include IpaA, IpaB, IpaC, IpaD, IpgD, IpgB, and VirA (2) and are reviewed in Refs. 3 and 4. Among these, the Ipa proteins are essential for entry (5). *Shigella* mutants unable to express IpaB, IpaC, or IpaD are not able to invade epithelial cells and IpaA mutants are impaired 10-fold (6–8). Exploring the molecular basis for how Ipa proteins alter the host cell cytoskeleton revealed that IpaB, IpaC, and IpaD elicit actin rearrangements at the site of bacterial attachment that are required for entry, whereas IpaA may promote the reorganization of these actin-rich structures (8).

One target of the Ipa proteins are members of the Rho family of GTPases (9, 10). Rho proteins act as molecular switches cycling between an active GTP-bound form and inactive GDP-bound state. Active Cdc42 and Rac trigger activation of the Arp2/3 complex and the formation of filopodia and lamellipodia, respectively (reviewed in Ref. 11). IpaC induces changes in the actin cytoskeleton, characteristic of active Cdc42 and Rac, and this effect is blocked by dominant negative versions of Cdc42 or Rac, or the Cdc42-binding domain of WASP suggesting that IpaC may up-regulate the activity of these GTPases (12). The mechanism for this is likely to involve phosphorylation of Crk by Abl tyrosine kinases and the subsequent activation of PAK (13, 14). Like Cdc42 and Rac, Rho activity is required for *Shigella* entry (9, 15). Increases in Rho activity stimulate numerous Rho effectors that could potentially remodel the actin cytoskeleton and drive increased contractility. For example, the RhoA effector Rho kinase increases phosphorylation of the myosin II regulatory light chain both directly and indirectly by inhibition of the myosin phosphatase (16, 17). The mechanism of Rho activation at the site of *Shigella* entry is unknown, but its activity is essential for the remodeling of the actin cytoskeleton and folding of membranes that occurs at the site of entry (9).

Another group of proteins that are localized to the site of bacterial entry and targeted by the *Shigella* effectors are adhesion receptors. IpaB binds to the extracellular domain of CD44, a transmembrane receptor that interacts with hyaluronic acid, and promotes *Shigella* entry (18, 19). Integrins are transmembrane adhesion receptors consisting of α and β subunits that serve as links between the extracellular matrix on the outside and the cytoskeleton on the inside. They are highly enriched at sites of bacterial entry and their expression level positively correlates with *Shigella* invasiveness (20). A complex of IpaB and IpaC bind to integrins (20) and may allow for transient adhesion

* This work was supported by National Institutes of Health Grants HL45100 and GM29860 (to K. B.) and CA111818 (to K. A. D.). The costs of publication of this article were defrayed in part by the payment of page charges. This article must therefore be hereby marked “advertisement” in accordance with 18 U.S.C. Section 1734 solely to indicate this fact.

[S] The on-line version of this article (available at <http://www.jbc.org>) contains supplemental Data A and B.

¹ To whom correspondence should be addressed: 4-470 Bowen Science Bldg., 51 Newton Rd., Iowa City, IA 52242. Tel.: 319-335-7882; Fax: 319-335-9570; E-mail: kris-demali@uiowa.edu.

of the bacterium with the cell surface to promote internalization (20). IpaA binds to vinculin, a protein present at the cytoplasmic face of integrins (8). The interaction of IpaA with vinculin increases recruitment of F-actin to vinculin (21, 22). A complex of vinculin and IpaA was shown to reduce F-actin sedimentation and decrease filament assembly on an EM grid leading the authors to suggest that this complex is important for “depolymerization” of actin filaments at the site of *Shigella* entry (21).

Here we explore how IpaA promotes the cytoskeletal rearrangements necessary for bacterial entry. We provide evidence that there is a loss of stress fibers in vinculin-null mouse embryo fibroblasts (MEFs)² expressing IpaA or in fibroblasts expressing a mutant of IpaA unable to bind vinculin. We find that cells expressing IpaA have elevated Rho activity and increased phosphorylation of myosin light chain resulting in increases in contractility that can be blocked by inhibitors of Rho kinase. Furthermore, we show that IpaA negatively regulates cell-matrix adhesion by interfering with recruitment of talin to the integrin cytoplasmic tail. The combination of IpaA-induced de-adhesion and increased contractility account for the loss of actin stress fibers and cell rounding observed in cells exposed to IpaA.

EXPERIMENTAL PROCEDURES

Reagents and Cell Lines—The vinculin-null mouse embryo fibroblasts (Vin^{-/-}; Ref. 23) were a generous gift of E. Adamson (Burnham Institute, La Jolla, CA). Vin^{-/-}, HeLa, and REF52s were maintained in Dulbecco’s modified Eagle’s medium + 10% fetal bovine serum as previously described (24). Human fibronectin was prepared as previously described (25). For the Rho kinase inhibitor studies, Y27632 (Calbiochem) was resuspended in Me₂SO, diluted to a final concentration of 750 nM in growth media for 30 min prior to and during microinjection.

Constructs—The GFP, Myc, and GST fusion proteins were constructed by PCR amplification of a cDNA of interest from pEC15 (26). Full-length IpaA was cloned using GGATCCATGCATAATGTAATAACTCAAGCGCCAACATTC as the upstream primer and GAATTCTTAATCCTTATTGATATCTTTAATACTTTTGATAGGG as the downstream primer. IpaA-(1–500) was constructed using the full-length upstream primer and GAATTCGGAGTTTGTACTTTTTTTGAAGC as the reverse primer and IpaA-(500–633) was constructed using GGATCCGGAACACAAGAACGAGAGTTACAGG as the forward primer and the full-length IpaA downstream primer. The resulting PCR products were cloned into the BglII-EcoRI sites of pEGFP-C1, or the BamHI-EcoRI sites of pGEX-T (Amersham Biosciences) or pCMV6, an amino-terminal Myc epitope-tagged eukaryotic expression vector (gift of Dr. Jonathan Chernoff, Fox Chase Cancer Center).

Rho Activity—Rho activity assays were performed as previously described (27) using the RhoA-binding domain of Rhotekin expressed as a GST fusion protein. The cDNA of the RhoA-binding domain (RBD) of Rhotekin comprising amino

acids 7–89 was cloned into the pGEX-2T vector and expressed as a GST fusion protein. REF52 cells expressing GFP, GFP-IpaA, GFP-IpaA-(1–500), or GFP-IpaA-(500–633) were washed twice in HEPES-buffered saline and lysed in 50 mM Tris, pH 7.6, 150 mM NaCl, 0.1% SDS, 0.5% sodium deoxycholate, 1% Triton X-100, and 10 mM MgCl₂. Thirty micrograms of GST-RBD attached to glutathione-Sepharose beads were incubated with clarified lysates for 30 min at 4 °C. The beads were washed four times in lysis buffer and the resulting products were analyzed using SDS-PAGE.

Immunoprecipitation and Western Blot Analysis—Cells were washed in HBS (20 mM HEPES, pH 7.4, 150 mM NaCl + 2 mM Na₃VO₄), and lysed in ice-cold EB (1% Triton X-100, 10 mM Tris, pH 7.4, 5 mM EDTA, 50 mM NaCl, 50 mM NaF, 20 μ g/ml aprotinin, 1 mM phenylmethylsulfonyl fluoride, 10 μ g/ml leupeptin, and 2 mM Na₃VO₄). Immunoprecipitation and immunoblotting were performed as previously described (24) using the following commercially available anti-sera: GFP (Roche and Clontech), Rho (BD Transduction Labs), phospho-Ser¹⁹ myosin light chain (BIOSOURCE), and myosin light chain (My-21; Sigma). Vinculin (G989) or talin (N681) were immunoblotted and immunoprecipitated with polyclonal antibodies raised against the full-length proteins as previously described (24, 28).

Immunofluorescence—Cells were fixed in 3.7% formaldehyde in phosphate-buffered saline, permeabilized in 0.5% Triton X-100, and washed in TBS (150 mM NaCl, 50 mM Tris, pH 7.6, 0.1% NaN₃). To visualize actin, cells were incubated with Texas Red-conjugated phalloidin (Molecular Probes) at 1:200 for 1 h at 37 °C, washed in universal buffer, and mounted on glass slides. Images were obtained as previously described using a Zeiss axiovert microscope. Images were acquired with a Hamamatsu ORCA-ER cooled charge-coupled device camera (Zeiss) and processed using Metamorph Image software (Universal Imaging). Vinculin was visualized using hVIN-1 (Sigma) at 1:400 followed by an anti-mouse Alexa 488-conjugated secondary antibody.

Microinjection—Cells were seeded onto glass bottom dishes (MATEK) 24 h prior to microinjection in Dulbecco’s modified Eagle’s medium + 10% fetal bovine serum. The dishes of cells were moved to a 37 °C incubation chamber for imaging. GST-IpaA was harvested from BL21(DE3) cells expressing a chaperone plasmid (Takara Mirus Bio) to facilitate recovery of soluble plasmid cultures induced with 0.33 mM isopropyl 1-thio- β -D-galactopyranoside overnight at room temperature. Bacterial cells were lysed, sonicated, and GST-IpaA was purified using glutathione-Sepharose beads. The purified products were concentrated using a microconcentrator and dialyzed into microinjection buffer (25 mM Tris, pH 7.3, 100 mM KCl, 5 mM MgCl₂, 1 mM EGTA), and injected at a concentration of 20 μ g/ml. The cells were monitored for 30 min using Zeiss axiovert inverted microscope equipped with a heat and humidified chamber and a Hamamatsu ORCA ER camera. Images were acquired as described above.

In Vitro Binding to Integrin Cytoplasmic Domain Constructs—The synthetic β 1A integrin cytoplasmic binding was obtained from Mark Ginsberg and purified as previously described (29). Platelet extracts were prepared as previously described (30). The

² The abbreviations used are: MEF, mouse embryo fibroblasts; GFP, green fluorescent protein; RBD, RhoA-binding domain; FACS, fluorescence-activated cell sorter.

IpaA Targets β 1 Integrins and Rho

platelet extracts were passed over a DEAE-52 column and the five column fractions most enriched for talin were pooled. The pH of these samples was adjusted to 7.5 and the salt concentration was adjusted to 50 mM. Nickel-nitrilotriacetic acid beads containing 50 μ g of purified β 1a integrin cytoplasmic domain were incubated with 300 μ l of talin-enriched platelet extracts in the presence of 0.2 or 2 μ g of GST or GST-IpaA. The resulting beads were washed four times in ice-cold phosphate-buffered saline + 0.5% Triton X-100, reconstituted in sample buffer, and subjected to Western blot analysis.

FACS Analysis—Subconfluent cultures of HeLa cells expressing Myc or Myc-IpaA were lifted from tissue culture dishes by incubation in phosphate-buffered saline + 0.6 mM EDTA for 15 min at 37 °C, washed, and stained with TS2/16 (American Type Tissue Culture Collection) or 12G10 (Chemicon) for 1 h at 4 °C. The cells were washed two times, stained with an anti-mouse IgG antibody conjugated with fluorescein (Chemicon) for 30 min at 4 °C, and washed three additional times. The stained cells were resuspended in Dulbecco's modified Eagle's medium + 0.2% fetal bovine serum, and analyzed in the University of North Carolina flow cytometry facility. For each wash step the cells were resuspended and pelleted in Dulbecco's modified Eagle's medium + 0.2% fetal bovine serum.

RESULTS

Upon contact with a host cell, *Shigella* triggers the formation of large membrane protrusions that arise from the host cell surface and engulf the bacterium. To form a structure that is productive for entry these densely packed actin-rich membrane protrusions reorganize. Both Rho and a complex of IpaA and vinculin have been implicated in the actin cytoskeletal rearrangements that occur during *Shigella* entry (9, 21). However, the mechanisms remain elusive. To investigate how IpaA affects the actin cytoskeleton, we cloned IpaA and studied the effects of recombinant IpaA expressed as a fusion with GFP in mammalian cells. We assessed whether our recombinant IpaA exhibited the same characteristics as IpaA purified from bacterial supernatants (21). For this, we examined coprecipitation of vinculin with GFP or GFP-IpaA immunoprecipitated from HeLa cell lysates. Consistently we immunoprecipitated much more GFP than GFP-IpaA from cell lysates but always detected vinculin binding only to GFP-IpaA and not to GFP alone (Fig. 1A). Previous findings suggested that IpaA purified from bacterial supernatants induced a loss of stress fibers when micro-injected into cells (21). We examined whether our GFP-IpaA was able to have a similar effect when transiently expressed. For these studies we utilized the REF52 cell line, which unlike HeLa cells, form robust actin stress fibers that are easily visualized. Under these conditions, $90 \pm 5\%$ of GFP-expressing cells formed large actin stress fibers that were easily visualized and indistinguishable from the untransfected cells (Fig. 1B). In contrast, $31 \pm 7\%$ of the cells expressing GFP-IpaA had no detectable stress fibers and $20 \pm 9\%$ of the cells showed a partial decrease in the number of actin stress fibers (Fig. 1C).

It was a bit surprising that such a large number of cells (*i.e.* $49 \pm 2\%$) would have relatively intact stress fibers. Sites where stress fibers terminate are known as focal adhesions. We considered whether disassembling the preexisting focal

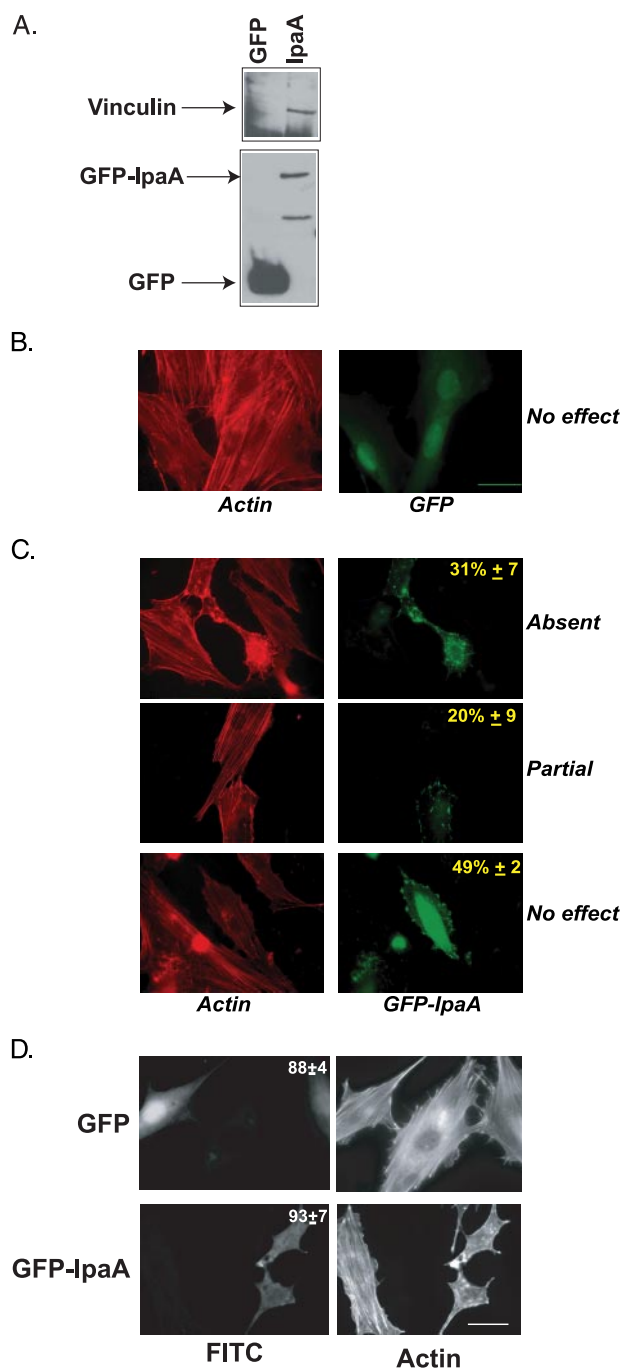


FIGURE 1. Recombinant IpaA binds to vinculin and induces a loss of actin stress fibers. A, recruitment of GFP-IpaA to vinculin. HeLa cells were transiently transfected with GFP or GFP-IpaA, allowed to recover for 18 h, lysed, and the fusion proteins were immunoprecipitated using an antibody against GFP. The resulting immunoprecipitates were subjected to Western blot analysis with antibodies against vinculin or GFP. Note the lower molecular weight band in the IpaA lane appears to be an incompletely transcribed product of GFP-IpaA. B–D, overexpression of GFP-IpaA induces a loss of actin stress fibers. REF52 cells transfected with GFP (B) or GFP-IpaA (C) were fixed, stained, and processed for fluorescence microscopy 18 h post-transfection, or D, trypsinized and replated on fibronectin-coated coverslips for 4 h. Right panels show GFP fluorescence and left panels were stained with rhodamine-conjugated phalloidin. Transfected cells were scored for a loss of stress fibers. The percentage of cells having no detectable actin stress fibers (absent), partial stress fibers (partial), or no loss of stress fibers (no effect) are indicated in the top right corner of each image. A cell was scored as having partial stress fibers if it had five or more visible stress fibers. Data are expressed as the mean \pm S.D. of three independent experiments. Bar = 50 μ m. FITC, fluorescein isothiocyanate.

adhesions might allow IpaA to access these sites better and have a greater effect. To test this possibility, focal adhesions were disassembled by resuspending cells by trypsinization followed by replating on fibronectin-coated coverslips for 4 h. Under these conditions, the percentage of IpaA-expressing cells lacking stress fibers significantly increased to $93 \pm 7\%$, whereas replating had relatively no effect on the stress fibers in GFP-expressing cells (Fig. 1D). Taken together, these results suggest that expression of recombinant IpaA induces a loss of actin stress fibers to a similar extent as microinjection of IpaA purified from bacterial supernatants.

Vinculin Is Not Required for the Effects of IpaA on the Actin Cytoskeleton—Earlier work implicated vinculin recruitment to IpaA as key for the loss of stress fibers and cell rounding observed in cells exposed to IpaA (21). To test the requirement for vinculin, we assessed the morphology and the integrity of actin stress fibers in vinculin-null ($Vin^{-/-}$) MEFs expressing GFP-IpaA or GFP alone (31). Surprisingly, the vinculin-null cells expressing GFP-IpaA showed a marked decrease in the number of stress fibers and were more rounded as compared with the GFP-expressing or untransfected control $Vin^{-/-}$ MEFs (Fig. 2A) suggesting that vinculin is not required for the effect on stress fibers by IpaA. IpaA had a slightly greater effect on stress fibers in the $Vin^{-/-}$ MEFs than in the REF52s, because $58 \pm 13\%$ of cells had no detectable actin stress fibers (Fig. 2B). These findings were not the result of prolonged exposure to IpaA because $Vin^{-/-}$ MEFs microinjected with GST-IpaA rounded very rapidly and did not appear to recover during the first 15 min of exposure (supplemental data). In contrast GST-injected cells were indistinguishable from the uninjected controls (supplemental data).

It is possible that in the absence of vinculin, the MEFs up-regulate a compensatory pathway that allows IpaA to induce a loss of stress fibers. To further explore whether vinculin is required for the effect of IpaA, we considered generating a mutant of IpaA that could not bind vinculin. This would allow us to examine the phenotype of the mutant IpaA when expressed in the presence of vinculin in REF52 cells. We mapped the vinculin binding site on IpaA using IpaA fragments expressed as fusions with GFP (Fig. 3A). Several overlapping fragments co-precipitated vinculin from cell lysates and identified the C-terminal 134 amino acids (residues 500–633) as the critical domain (Fig. 3B). We next assessed the ability of GFP fusions with either one of these two IpaA fragments to induce a loss of stress fibers and cell rounding in REF52 cells (Fig. 3C) or $Vin^{-/-}$ MEFs (Fig. 2). In both cell lines, the fragment of IpaA that bound vinculin (IpaA-(500–633)) behaved similarly to GFP. Neither cell line exhibited a significant decrease in actin stress fibers (Figs. 2 and 3C). In some instances the number and intensity of stress fibers in the GFP-IpaA-(500–633) expressing cells appeared to be increased (Figs. 2A and 3C). In contrast, cells exposed to the fragment of IpaA lacking the vinculin binding site (GFP-IpaA-(1–500)) behaved similarly to full-length GFP-IpaA, and exhibited a noticeable decrease in the number of actin stress fibers (Figs. 2 and 3C). Taken together these results demonstrate that vinculin is not required for IpaA-induced cytoskeletal rearrangements.

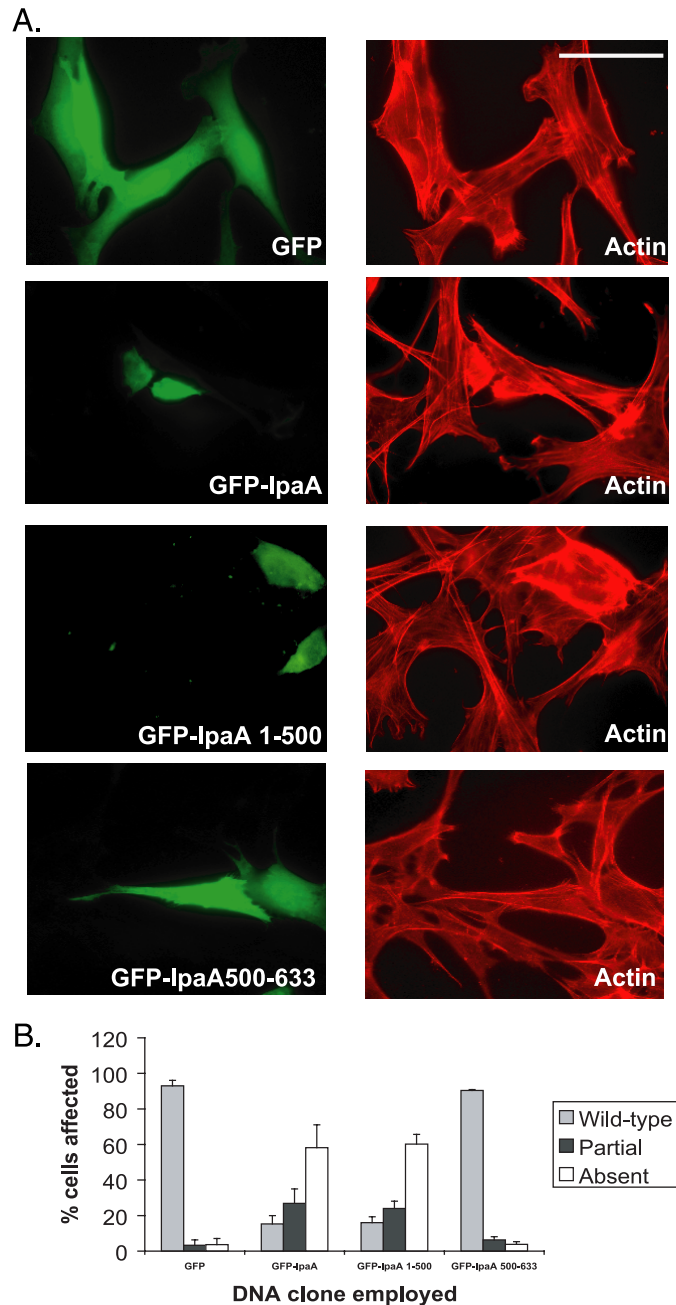


FIGURE 2. Vinculin is not required for the effects of IpaA. A, vinculin-null MEFs expressing GFP, GFP-IpaA, GFP-IpaA-(1–500), or GFP-IpaA-(500–633) were fixed, permeabilized, and stained with Texas Red-conjugated phalloidin (actin, right panels). Representative images of the GFP fluorescence are shown in the left panels. B, cells expressing GFP or the GFP-IpaA clone denoted and exhibiting a complete loss (absent), partial decrease (partial), or wild-type levels of stress fibers were quantitated and expressed as a percentage of total cells.

These findings led us to pursue alternative mechanisms for how IpaA induces a loss of actin stress fibers. The small GTPase Rho appeared as a likely candidate because inhibiting Rho leads to a loss of stress fibers and focal adhesions. We measured Rho activity in cells expressing GFP-IpaA. Contrary to what we expected, we found that cells expressing GFP-IpaA had elevated RhoGTP levels when compared with the GFP-expressing cells (Fig. 4A). This effect could be mapped to the first 500 amino acid residues of IpaA because cells expressing GFP-

IpaA Targets β 1 Integrins and Rho

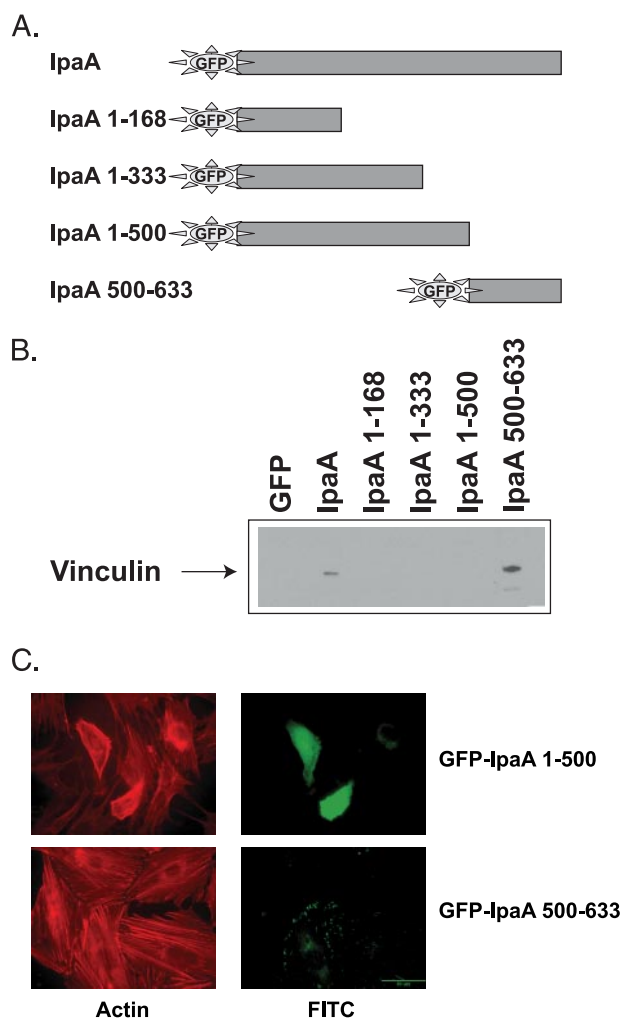


FIGURE 3. Mapping the vinculin binding site on IpaA. *A*, linear schematic is shown of IpaA and the fragments of IpaA as fusion proteins of GFP. *B*, the fusion proteins were expressed in HeLa cells for 18 h, immunoprecipitated from cell lysates using an antibody against GFP, prepared, and blotted for vinculin as described in the legend to Fig. 1. *C*, REF52 cells expressing GFP-IpaA-(1–500) or GFP-IpaA-(500–633) for 18 h were analyzed as described in the legend of Fig. 1. Bar = 50 μ m.

IpaA-(1–500), but not GFP-IpaA-(500–633), had high Rho activity (Fig. 4A). One downstream effector of Rho is Rho kinase, which promotes myosin light chain phosphorylation thereby stimulating actomyosin contractility (16, 17). To determine whether increased contractility is a consequence of increased Rho activity in cells expressing IpaA, we examined myosin light chain phosphorylation in lysates harvested from GFP or GFP-IpaA-expressing cells. In comparison to the GFP control cells, myosin light chain phosphorylation was increased in lysates harvested from GFP-IpaA or GFP-IpaA-(1–500) (Fig. 4B). The GFP-IpaA-(500–633) expressing cells showed no change in the levels of phosphorylated myosin light chain when compared with the GFP controls (Fig. 4B). Hence IpaA activates Rho and increases the phosphorylation of myosin light chain independently of binding to vinculin.

If IpaA-induced cell rounding is the result of increased actomyosin contractility stimulated by elevated Rho activity, then inhibiting this pathway should prevent cell rounding. To test this, we incubated cells with a low dose of the Rho kinase inhib-

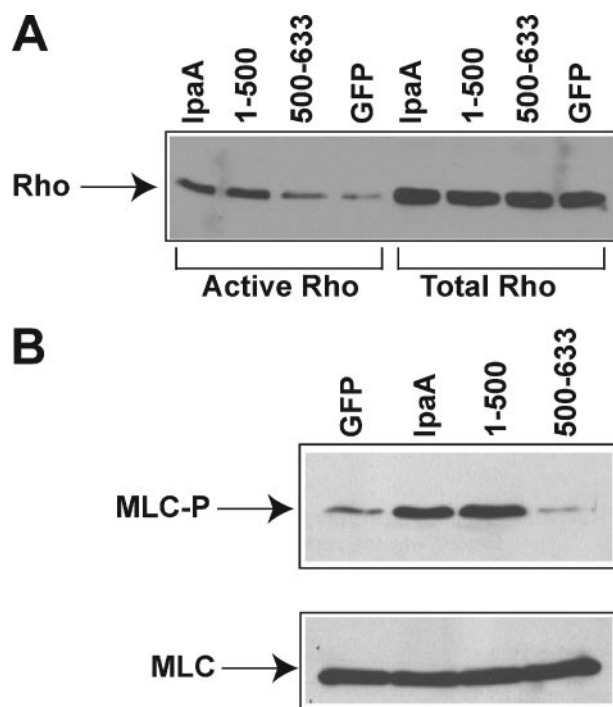


FIGURE 4. IpaA increases Rho activity and myosin light chain phosphorylation. Lysates from REF52 cells expressing GFP, GFP-IpaA, GFP-IpaA-(1–500) (1–500), or GFP-IpaA-(500–633) (500–633) were harvested. *A*, the amount of GTP-bound Rho was measured using a GST fusion protein containing the Rho-binding domain of Rhotekin (RBD) that selectively binds only GTP-bound Rho. GST-RBD precipitations were probed with a monoclonal antibody against Rho. Rho immunoblots show Rho protein levels in the pulldowns (Active Rho) or a sample of total cell lysates (total Rho). *B*, the lysates were separated by SDS-PAGE and subjected to Western blot analysis with antibodies that recognize phosphorylated myosin light chain serine 19 (MLC-P) or total myosin light chain (MLC).

itor Y27632 that inhibits Rho kinase activity without inducing gross structural changes in cell morphology. These cells were microinjected with GST or GST-IpaA. We found that cells preincubated with Y27632 and injected with GST-IpaA resembled the GST-injected cells, in that they did not round during the first 30 min of exposure (supplemental Data B). This confirmed that IpaA-dependent cell rounding is the result of Rho-mediated increased contractility.

IpaA Induces the Disassembly of Focal Adhesions—Cells expressing GFP-IpaA appeared less well spread, consistent with the idea that IpaA may be decreasing integrin-mediated cell adhesion. To test this hypothesis, we used FACS analysis to determine whether IpaA affects the affinity or amount of β 1 integrin on the cell surface using the monoclonal antibodies 12G10 and TS216 (32). Myc-IpaA-expressing cells showed a marked decrease in active integrins on the cell surface as compared with the Myc only expressing cells (Fig. 5A). The total levels of integrin on the cell surface were not altered in the two cell types (Fig. 5B) suggesting that IpaA induces de-adhesion by decreasing integrin affinity for its ligands.

Control of integrin affinity for ligands is regulated by talin recruitment to the cytoplasmic domain (33). This triggers conformational changes in the integrin associated with a conversion from a low to a high affinity for ligands (34) and the subsequent recruitment of other cytoskeletal proteins to this site. Because IpaA decreases integrin affinity for ligands, we assessed

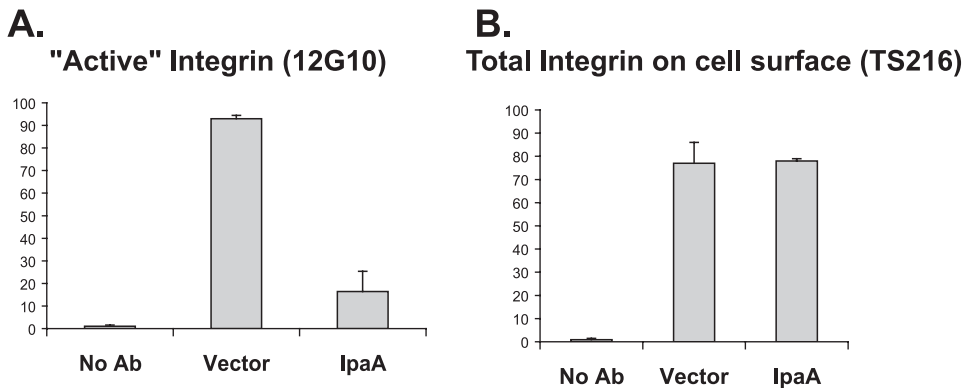


FIGURE 5. IpaA decreases integrin affinity for ligands. Thirty hours post-transfection, HeLa cells expressing pCMV6 (*Vector*) or pCMV6IpaA (*IpaA*) were washed and lifted from tissue culture surfaces using phosphate-buffered saline + EDTA. The cells were stained with 12G10 (*A*, *Active Integrin*) or TS216 (*B*, *Total Integrin*) followed by a fluorescein isothiocyanate-conjugated anti-mouse secondary antibody. Positive cells were scored using FACS analysis and plotted as percentage of the control. Parental HeLa cells were stained with secondary antibody alone (*No Ab*) and used as a negative control.

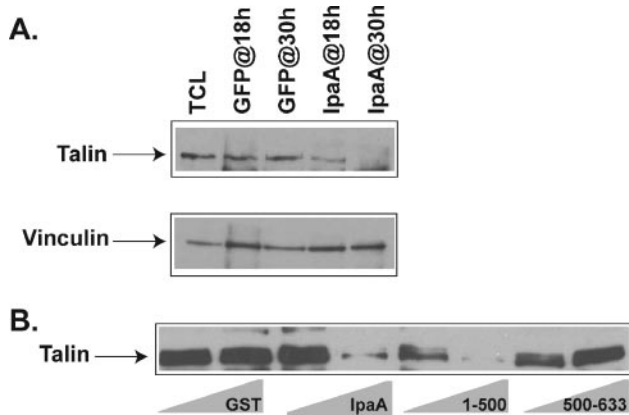


FIGURE 6. IpaA prevents talin association with vinculin and integrin cytoplasmic domain. *A*, prolonged exposure to IpaA decreases talin recruitment to vinculin. Vinculin immunoprecipitates were recovered from HeLa cells expressing GFP or GFP-IpaA (*IpaA*) at short (18 h) or long (30 h) time periods post-transfection. The immunoprecipitates were washed, separated using SDS-PAGE, and analyzed using Western blotting with antibodies against vinculin or talin. *B*, IpaA disrupts talin recruitment to the integrin cytoplasmic domain. β 1a integrin cytoplasmic domains attached to Sepharose beads were incubated with talin-rich human platelet extracts and either 0.2 μ g or 2.0 μ g of GST, GST-IpaA, GST-IpaA-(1–500), or GST-IpaA-(500–633). The beads were washed and the resulting products were analyzed by SDS-PAGE and Western blotting with antibodies against talin.

whether it perturbs talin binding to vinculin or the integrin cytoplasmic domain itself. We first explored coprecipitation of talin with vinculin in immunoprecipitates from cells expressing GFP or GFP-IpaA. In comparison with the talin recruitment to vinculin in the GFP-expressing cells, we noticed a slight decrease in the amount of talin recruited to vinculin in cells expressing GFP-IpaA 18 h post-transfection (Fig. 6A). In cells 30 h post-transfection, GFP-IpaA, but not GFP alone, resulted in a decrease in the level of talin coprecipitating with vinculin (Fig. 6A).

We considered whether talin binding to the integrin cytoplasmic domain was affected under these conditions. Two possibilities exist. Talin recruitment to the intracellular domain of integrin β subunit is lost or talin remains bound. Because the affinity of integrins for talin is very low and hard to detect in conventional integrin immunoprecipitates, we took advantage

of a recombinant integrin construct that mimics four clustered integrin cytoplasmic domains (29). His-tagged versions of these integrin cytoplasmic domain mimetics were produced in bacteria, purified and attached to nickel-nitrilotriacetic acid beads. We found that this construct readily recovered talin from platelet extracts (data not shown) and addition of varying concentrations of GST or GST-IpaA-(500–633) to the platelet extracts did not interfere with talin binding (Fig. 6B). In contrast addition of even low amounts of GST-IpaA (0.2 μ g) to the extracts decreased talin recruitment and high doses (2 μ g) of GST-

IpaA or GST-IpaA-(1–500) blocked binding of talin to the integrin cytoplasmic domain (Fig. 6B). These findings suggest that IpaA disrupts cell-matrix adhesions by interfering with the recruitment of talin to the integrin cytoplasmic domain.

DISCUSSION

In this study we examined the mechanism for IpaA-induced cytoskeletal rearrangements. Earlier work suggested that IpaA binds to vinculin and induces increased recruitment of F-actin to vinculin and depolymerization of actin stress fibers (8, 21). Here we show that vinculin is not required for the effects of IpaA on the actin cytoskeleton. Our data do not suggest that the interaction of vinculin is unimportant for *Shigella*, but that it is not needed for the disruption of stress fibers or cell rounding that occur in response to IpaA. Rather we present evidence that IpaA activates the small GTPase Rho leading to elevated myosin light chain phosphorylation and increased contractility. Furthermore, we find that IpaA decreases cell-matrix adhesion and the mechanism for this involves preventing talin from binding to the integrin β 1 cytoplasmic domain. Together these observations lead us to suggest that one way that IpaA induces cytoskeletal rearrangements necessary for *Shigella* entry is to coordinately regulate the activity of Rho and the disassembly of cell-matrix adhesions. Moreover, the result of these two effects, namely weakened adhesion and increased contractility account for the loss of actin stress fibers and cell rounding observed in cultured cells into which IpaA has been introduced.

At the outset of this work we were motivated to determine how IpaA binding to vinculin induces a loss of stress fibers. Surprisingly, we found that the loss of stress fibers and cell rounding occur in mouse embryo fibroblasts that lack vinculin (Fig. 2), as well as in normal cells expressing a mutant of IpaA that is unable to bind vinculin (Fig. 3C and supplemental data). These findings differ from earlier work indicating that vinculin is required for the effects of IpaA (21). One difference between our work and the earlier work is that the studies presented here were performed using vinculin-null mouse embryo fibroblasts and the earlier work utilized cancer cell lines that lack detectable levels of vinculin expression. It is possible that there are some compensatory pathways that are up-regulated in the vin-

IpaA Targets β 1 Integrins and Rho

culin-null mouse embryo fibroblasts that may account for some of the differences between our work and the earlier studies. However, our observation that IpaA exerts its effects on the actin cytoskeleton in the absence of an intact vinculin binding site when expressed in "normal" cell lines strongly argues against a major role for vinculin in the IpaA-mediated loss of actin stress fibers.

These findings raise the question as to what is the relevance of IpaA binding to vinculin at the site of *Shigella* entry. Previous studies and our work here demonstrate that vinculin is readily recruited to IpaA (Refs. 8 and 21, and Fig. 1). We considered the possibility that vinculin might localize IpaA to the proper locale at the site of entry. However, this seems very unlikely because vinculin recruitment to the site of entry is both Rho- and IpaA-dependent (8, 10). Alternatively, vinculin binding may be needed for some as yet to be identified functions of IpaA. For example, IpaA shares some homology with the *Salmonella* entry effector SipA, which has several biological functions. It will be interesting to determine whether IpaA has similar activities to SipA and if these activities are affected by the interaction of IpaA with vinculin. It is also possible that recruitment of IpaA to vinculin affects a later step of bacterial invasion, such as the intercellular motility of *Shigella*. Vinculin has been shown to be cleaved upon *Shigella* entry exposing ActA homolog binding sites and increasing bacterial motility 3-fold (35). Finally, there is some evidence that suggests that vinculin stabilizes the maturation of small integrin-talin complexes into more stable adhesions (36) raising the intriguing possibility that IpaA binds vinculin to sequester it away from an integrin-containing complex. If IpaA hijacks vinculin in this manner, IpaA would be expected to promote the turnover of the adhesion structure. This would confer upon IpaA an additional level with which it is able to regulate adhesion complexes and actin cytoskeletal rearrangements during *Shigella* invasion.

Rather than vinculin mediating the effects of IpaA on the cytoskeleton, we found that IpaA activates Rho (Fig. 4). At first, high Rho activity seemed an unlikely candidate for mediating the effect of IpaA because elevated Rho activity triggers the formation of stress fibers and focal adhesions. However, in situations when adhesion is weak, such as in IpaA-expressing cells (Figs. 5 and 6), the increased contractility from high Rho activity would lead to cell rounding and a loss of stress fibers. This is analogous to what happens to a cell that is rounded during mitosis (37). How IpaA activates Rho is not known. It has no known sequence homology to guanine nucleotide exchange factors for members of the Rho family of GTPases or other bacterial proteins that serve as guanine nucleotide exchange factors suggesting that it is unlikely that IpaA acts alone as a guanine nucleotide exchange factor. The possibility that IpaA activates an endogenous guanine nucleotide exchange factor for Rho or inhibits a Rho GTPase activating protein will be investigated in future studies.

We also found that IpaA induces a loss of integrin-mediated adhesion. Cells expressing GFP-IpaA had a lower affinity for integrin ligands than GFP expressing cells and recruitment of talin to the integrin cytoplasmic domain was impaired. Unlike other bacteria, *Shigella* preferentially enters polarized epithelial cells at the basolateral pole, a region rich in α 5 β 1 integrins (15),

and this effect is mimicked in cell culture where *Shigella* invade more efficiently at focal adhesions (20). Hence decreased adhesion at the site of *Shigella* entry is likely to be a late step in the invasion process and is consistent with the observation that IpaA facilitates entry but is not required (8).

It is striking that the *Shigella* Ipa proteins target both sides of integrin-type adhesions. Thus, IpaB and IpaC bind to the extracellular domain of integrins and have been implicated in attachment of the bacterium to host cells and subsequent internalization (20). On the other hand, IpaA binds to vinculin (8), a protein at the cytoplasmic face of integrin-mediated adhesions, and we show here that it blocks the interaction of talin with integrin cytoplasmic domains. The effects appear at first sight to be antagonistic, initially promoting adhesion and then disrupting it. This leads us to speculate that the bacterium may be exploiting host mechanisms for internalization of adhesion complexes. Recent evidence indicates that focal adhesions (sites of integrin engagement and clustering) are turned over by an endocytic mechanism (38). Little is known about how integrins are internalized, but it is likely that they must first be disengaged from their cytoskeletal attachments. This would be favored by dissociation of talin from the cytoplasmic domain. Consequently, it is possible that a complex of IpaB and IpaC initiate the internalization process and the inhibition of talin binding to integrins by IpaA may promote a later step in endocytosis and contribute to the uptake of bacteria.

Acknowledgments—We thank Mark Ginsberg for the generous gift of the β 1a recombinant integrin cytoplasmic domain construct, Malabi Ventakersan for the pEC15 plasmid encoding IpaA, and Eileen Adamson for the vinculin-null mouse embryo fibroblasts.

REFERENCES

1. Blocker, A., Komoriya, K., and Aizawa, S. (2003) *Proc. Natl. Acad. Sci. U. S. A.* **100**, 3027–3030
2. Ohya, K., Handa, Y., Ogawa, M., Suzuki, M., and Sasakawa, C. (2005) *J. Biol. Chem.* **280**, 24022–24034
3. Cossart, P., and Sansonetti, P. J. (2004) *Science* **304**, 242–248
4. Page, A. L., Fromont-Racine, M., Sansonetti, P., Legrain, P., and Parsot, C. (2001) *Mol. Microbiol.* **42**, 1133–1145
5. Parsot, C., Menard, R., Gounon, P., and Sansonetti, P. J. (1995) *Mol. Microbiol.* **16**, 291–300
6. Menard, R., Sansonetti, P. J., and Parsot, C. (1993) *J. Bacteriol.* **175**, 5899–5906
7. Sasakawa, C., Kamata, K., Sakai, T., Makino, S., Yamada, M., Okada, N., and Yoshikawa, M. (1988) *J. Bacteriol.* **170**, 2480–2484
8. Tran Van Nhieu, G., Ben-Ze'ev, A., and Sansonetti, P. J. (1997) *EMBO J.* **16**, 2717–2729
9. Adam, T., Giry, M., Boquet, P., and Sansonetti, P. (1996) *EMBO J.* **15**, 3315–3321
10. Watarai, M., Kamata, Y., Kozaki, S., and Sasakawa, C. (1997) *J. Exp. Med.* **185**, 281–292
11. DeMali, K. A., and Burridge, K. (2003) *J. Cell Sci.* **116**, 2389–2397
12. Tran Van Nhieu, G., Caron, E., Hall, A., and Sansonetti, P. J. (1999) *EMBO J.* **18**, 3249–3262
13. Burton, E. A., Plattner, R., and Pendergast, A. M. (2003) *EMBO J.* **22**, 5471–5479
14. Abassi, Y. A., and Vuori, K. (2002) *EMBO J.* **21**, 4571–4582
15. Mounier, J., Vasselon, T., Hellio, R., Lesourd, M., and Sansonetti, P. J. (1992) *Infect. Immun.* **60**, 237–248
16. Amano, M., Ito, M., Kimura, K., Fukata, Y., Chihara, K., Nakano, T., Matsuura, Y., and Kaibuchi, K. (1996) *J. Biol. Chem.* **271**, 20246–20249

17. Kimura, K., Ito, M., Amano, M., Chihara, K., Fukata, Y., Nakafuku, M., Yamamori, B., Feng, J., Nakano, T., Okawa, K., Iwamatsu, A., and Kaibuchi, K. (1996) *Science* **273**, 245–248
18. Lafont, F., Tran Van Nhieu, G., Hanada, K., Sansonetti, P., and van der Goot, F. G. (2002) *EMBO J.* **21**, 4449–4457
19. Skoudy, A., Mounier, J., Aruffo, A., Ohayon, H., Gounon, P., Sansonetti, P., and Tran Van Nhieu, G. (2000) *Cell Microbiol.* **2**, 19–33
20. Watarai, M., Funato, S., and Sasakawa, C. (1996) *J. Exp. Med.* **183**, 991–999
21. Bourdet-Sicard, R., Rudiger, M., Jockusch, B. M., Gounon, P., Sansonetti, P. J., and Nhieu, G. T. (1999) *EMBO J.* **18**, 5853–5862
22. Chen, H., Cohen, D. M., Choudhury, D. M., Kioka, N., and Craig, S. W. (2005) *J. Cell Biol.* **169**, 459–470
23. Xu, W., Coll, J. L., and Adamson, E. D. (1998) *J. Cell Sci.* **111**, 1535–1544
24. DeMali, K. A., Barlow, C. A., and Burridge, K. (2002) *J. Cell Biol.* **159**, 881–891
25. Ruoslahti, E., Hayman, E. G., Pierschbacher, M., and Engvall, E. (1982) *Methods Enzymol.* **82**, 803–831
26. Venkatesan, M. M., Buysse, J. M., and Kopecko, D. J. (1988) *Proc. Natl. Acad. Sci. U. S. A.* **85**, 9317–9321
27. Arthur, W. T., Petch, L. A., and Burridge, K. (2000) *Curr. Biol.* **10**, 719–722
28. Rochlin, M. W., Chen, Q. M., Tobler, M., Turner, C. E., Burridge, K., and Peng, H. B. (1989) *J. Cell Sci.* **92**, 461–472
29. Pfaff, M., Liu, S., Erle, D. J., and Ginsberg, M. H. (1998) *J. Biol. Chem.* **273**, 6104–6109
30. Turner, C. E., and Burridge, K. (1989) *Eur. J. Cell Biol.* **49**, 202–206
31. Xu, W., Baribault, H., and Adamson, E. D. (1998) *Development* **125**, 327–337
32. Mould, A. P., Garratt, A. N., Askari, J. A., Akiyama, S. K., and Humphries, M. J. (1995) *FEBS Lett.* **363**, 118–122
33. Tadokoro, S., Shattil, S. J., Eto, K., Tai, V., Liddington, R. C., de Pereda, J. M., Ginsberg, M. H., and Calderwood, D. A. (2003) *Science* **302**, 103–106
34. Kim, M., Carman, C. V., and Springer, T. A. (2003) *Science* **301**, 1720–1725
35. Laine, R. O., Zeile, W., Kang, F., Purich, D. L., and Southwick, F. S. (1997) *J. Cell Biol.* **138**, 1255–1264
36. Papagrigoriou, E., Gingras, A. R., Barsukov, I. L., Bate, N., Fillingham, I. J., Patel, B., Frank, R., Ziegler, W. H., Roberts, G. C., Critchley, D. R., and Emsley, J. (2004) *EMBO J.* **23**, 2942–2951
37. Maddox, A. S., and Burridge, K. (2003) *J. Cell Biol.* **160**, 255–265
38. Ezratty, E. J., Partridge, M. A., and Gundersen, G. G. (2005) *Nat. Cell Biol.* **7**, 581–590